Research article

Resistance to crizotinib in a cMET gene amplified tumor cell line is associated with impaired sequestration of crizotinib in lysosomes

Nele Van Der Steen[1,2,3], Richard J Honeywell[3], Henk Dekker[3], Johan Van Meerloo[4], Jeroen Kole[5], René Musters[5], Rob Ruijtenbeek[6], Christian Rolfo[7], Patrick Pauwels[1,2], Godefridus J Peters[3], Elisa Giovannetti[3,8,*]

[1] Center for Oncological Research, University of Antwerp, Antwerp, Universiteitsplein 1, 2610 Wilrijk, Belgium
[2] Department of Pathology, Antwerp University Hospital, Antwerp, Universiteitsplein 1, 2610 Wilrijk, Belgium
[3] Department of Medical Oncology, VU University Medical Center, De Boelelaan 1117, 1081HV, Amsterdam, The Netherlands
[4] Department of Pediatric Oncology/Hematology, VU University Medical Center, De Boelelaan 1117, 1081HV, Amsterdam, The Netherlands
[5] Department of Physiology, VU University Medical Center, De Boelelaan 1117, 1081HV, Amsterdam, The Netherlands
[6] Wolvenhoek 10, 5211 HH 's-Hertogenbosch, The Netherlands
[7] Phase I - Early Clinical Trials Unit, Oncology Department, Antwerp University Hospital, Antwerp, Universiteitsplein 1, 2610 Wilrijk, Belgium
[8] Cancer Pharmacology Lab, AIRC Start-Up Unit, University of Pisa, Cisanello Hospital, via Paradisa 2, 56124 Pisa, Italy

*Correspondence: elisa.giovannetti@gmail.com (Elisa Giovannetti)

Abstract
Several cMET inhibitors have been developed as novel therapeutic candidates and are under investigation in clinical trials. New preclinical models to study mechanisms underlying resistance to these targeted agents are essential, as resistance acquired during treatment may lead to relapse. The squamous non-small-cell lung cancer (NSCLC) cell line EBC-1 harbors a cMET gene amplification and is sensitive to the cMET inhibitor crizotinib. Here, through multiple step selection with gradually increasing concentrations of crizotinib we established a resistant clone of these cells, termed EBC-CR. A tyrosine kinase activity assay did not show increased signaling of a bypassing pathway or renewed activity of cMET after crizotinib treatment. However, the pH-sensitive pHRodo Green AM probe showed increased acidification of the cytoplasm and lysosomes of EBC-CR cells. Live cell fluorescence imaging also showed an increase in lysosomal number after crizotinib treatment, and the intracellular concentration of crizotinib was significantly lower in crizotinib-resistant EBC-CR cells as compared to the drug sensitive parental EBC-1 cells. These findings suggest that the impaired accumulation of crizotinib in EBC-CR cells, together with the increased acidification of the lysosomes, contributes to crizotinib resistance in cMET-amplified NSCLC cells. In conclusion, the present research identified a novel mechanism used by cancer cells to confer resistance to cMET inhibition. These results prompt future studies for the establishment of innovative therapeutic strategies to overcome resistance to cMET kinase inhibitors by modulation of lysosomal acidification.

Keywords
C-MET; Crizotinib; Resistance; Lysosomes

Submitted: November 3, 2017; **Revised:** February 4, 2018; **Accepted:** February 9, 2018

1. Introduction

The cMET receptor is encoded by the cMET proto-oncogene. Binding of its ligand HGF (hepatocyte growth factor) leads to the activation of downstream signaling pathways, amongst which are MAPK cascades, PI3K/Akt signaling and STAT3 [1]. Signaling through cMET is involved in several oncogenic processes like cell motility, invasiveness and metastasis [1]. In non-small cell lung cancer (NSCLC), cMET is both known as an oncogenic driver and a drug resistance mechanism against targeted therapies. Amplification of the cMET gene [1] or exon 14 skipping [2] are both known biomarkers for response to anti-cMET targeted therapies. The first generation cMET tyrosine kinase inhibitor (cMET-TKI) crizotinib is active against NSCLC cells harboring cMET gene amplification and/or cMET exon 14 skipping [2–4]. In EGFR (epidermal growth factor receptor) mutated NSCLC, cMET gene amplification is mainly

known as a resistance mechanism to EGFR-TKIs [5]. Amplification of the cMET gene occurs in approximately 10-20% of resistant tumors [5].

Drug resistance against targeted therapies occurs after one year of treatment on average. A first mechanism is the emergence of secondary/tertiary mutations. An example hereof is the D1228N secondary mutation in cMET. This mutation confers resistance to crizotinib in cMET exon 14 skipping-positive NSCLC [6]. Another example includes mutations in EGFR, where the T790M mutation confers resistance to the first generation EGFR-TKIs [7], whereas the C797S mutation confers resistance to the third generation of EGFR-TKIs [8]. A second mechanism is the activation of a parallel signaling pathway through the amplification of another oncogene (e.g. cMET amplification confers resistance to EGFR-TKI-treated NSCLC [5]. Thirdly, activation of downstream signaling can also lead to drug resistance, irrespective of the activity of the upstream

receptor. A well-known example hereof is KRAS. Additional mutations in KRAS, leading to its continuous activation, bypass EGFR-inhibition by causing continuous downstream signaling [9]. In the case of EGFR-mutated NSCLC, a switch in histology from adenocarcinoma to small cell lung cancer can also confer resistance against EGFR-TKIs [10].

In the case of a hydrophobic weak-base anticancer drug, the lysosomes can play a role in resistance through passive ion-trapping [11]. In short, hydrophobic weak-base drugs are able to freely cross the plasma membrane and the lysosomal membrane. Once they cross the lysosomal membrane, the acidic pH inside the lysosomes triggers the protonation of the drug, thus preventing the drug from crossing the lysosomal membrane again. The lysosomes sequester or trap these drugs inside, therefore the drugs cannot reach their assumed target (e.g. the intracellular domain of a receptor) and cannot exert their cytotoxic function, which leads to cellular drug resistance [11–13]. Lysosomal drug sequestration triggers lysosomal biogenesis through the activation of the CLEAR pathway (Coordinated lysosomal expression and regulation) [14], and promotes lysosomal exocytosis [15].

In this study we aimed to unravel the mechanism underlying resistance to crizotinib in tumor cells harboring cMET gene amplification, evaluate both key signaling pathways and the potential role of lysosomes.

2. Materials and methods

2.1. Cell lines and therapeutics

The EBC-1 cell line was purchased from JCRB and cultured in DMEM supplemented with 10% fetal bovine serum (BioWest, Nuaillé, France), 20 mM HEPES pH 7.3, 100 IU/ml penicillin and 100 µg/ml streptomycin. All culture media were purchased from Lonza (Breda, Netherlands) except when otherwise stated. Cells were maintained in 25-75 cm^2 flasks (Greiner Bio-One GmbH, Frickenhausen, Germany) and incubated at 37°C in a humidified atmosphere of 5% CO_2.

Crizotinib was purchased from SelleckChem (Houston, USA), dissolved in DMSO, aliquoted out and stored at −80°C until further use. Immediately before use, crizotinib was diluted in PBS.

2.2. Sulforhodamine B assay

Cell growth inhibition was determined using the sulforhodamine B assay (SRB) [16]. Briefly, cells were seeded in 96-well flat bottom plates (Greiner Bio-One GmbH, Frickenhausen, Germany) and were allowed to attach overnight. Next day, cells were treated with a range of crizotinib concentrations (0-5 µM). A dilution of 0.1% DMSO served as control. After 72 h, cells were fixed with 50% trichloroacetic acid, incubated at 4°C for one hour and washed 5 times with water. Cells were stained with a 0.4% SRB solution in 1% acetic acid and incubated for 15 min at room temperature. To remove unbound stain, the plates were washed 5 times with 1% acetic acid and were allowed to dry. Cellular SRB stain was dissolved in 10 mM Tris-base and the optical density was determined at 540 nm with the HTX Synergy microplate reader (BioTek). The IC_{50} concentration of crizotinib was determined with Graphpad Prism (v5).

2.3. Establishment of crizotinib-resistant cells

Parental EBC-1 cells were maintained in a 25 cm^2 flasks and first treated with a crizotinib concentration representing the IC_{50} value. The growth medium was refreshed once a week until cells started to grow at the parental growth rate. Drug concentrations were increased when cells continued to proliferate. When cells were growing normally at a concentration of 1 µM of crizotinib, drug treatment was terminated and cells were grown at least four weeks in crizotinib-free medium prior to SRB assays. Next, the crizotinib IC_{50} values were determined while comparing the parental EBC-1 cell line with its EBC-CR daughter subline.

2.4. Tyrosine kinase activity array

Analysis of tyrosine kinase inhibition was performed as previously described [17]. Cells were seeded in 25 cm^2 flasks and treated for 24 h with their respective IC_{50} concentrations of crizotinib (25 nM for the EBC-1 and 7 µM for the EBC-CR) or 0.1% DMSO as a vehicle control. Lysis buffer was made by adding phosphatase and protease inhibitors (Thermo Scientific, Rockford, IL) to M-PER buffer (mammalian protein extraction reagent, pH 7.6) (Thermo Scientific, Rockford, IL). Cells were lysed on ice and harvested using a cell scraper. Lysates were spun at 10,000 × g for 15 min at 4°C, supernatant was collected and either immediately used or stored at −80°C until analysis. 5 µg aliquot of total protein lysate was incubated with reaction buffer 1×ABL buffer (Westburg), 100 µM ATP (Sigma-Aldrich), and fluorescein-labeled antibody PY20 (Exalpha, Maynard, MA). The arrays were blocked with 2% BSA before loading of the sample and next incubated at 30°C for 60 cycles on a Pam-Station 12 (Pamgene International, 's Hertogenbosch, The Netherlands). A 12-bit CCD camera was used for fluorescence imaging, monitoring the fluorescence in real-time. Spot intensities and time-resolved curves were fit to calculate the amount of phosphorylation by Bionavigator software version 6.1 (PamGene International).

2.5. Intracellular drug concentration

The intracellular concentration of crizotinib was determined as previously described [18]. In brief, cells were seeded and treated for 24 h with 5 µM crizotinib. Bafilomycin A1 was used to disrupt the acidic lysosomal pH and thus prevent lysosomal sequestration of crizotinib. A final concentration of 50 nM bafilomycin A1 was added to the cells 30 min prior to crizotinib treatment. Next, cells were sedimented by centrifugation and washed 3 times with PBS. Pellets were snap-frozen and stored at −80°C until further analysis. After addition of 160 µl of cold phosphate buffer, cell pellets were homogenized and protein concentration was determined with the Bio-rad Bradford protein assay according to manufacturer's instructions. A sample of 100 µl was added to 400 µl acetonitrile, incubated for 20 min on ice, vortexed and centrifuged (21,000 × g, 10 min at 4°C). Next, 100 µl were used for LC injection. Statistical analysis was performed with graphpad prism v5 using one-way ANOVA with Tukey post-hoc testing.

2.6. Live cell imaging

Cells were plated in a chambered cover glass (#1.5, Nunc Lab-Tek, Thermo Scientific, Rockford, IL) and treated for 24 h with 5 µM crizotinib or 0.1% DMSO as the vehicle control. The next day, the growth medium was replaced by an IMDM medium devoid of a pH
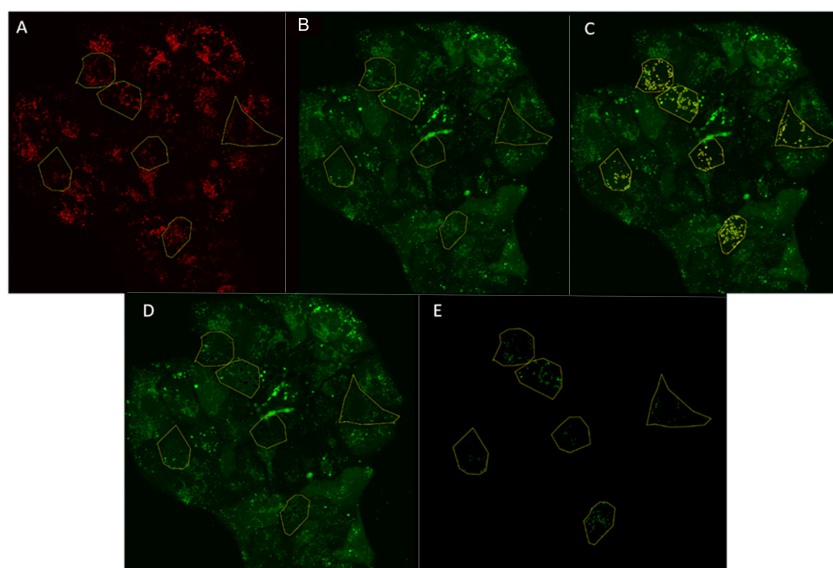
Fig. 1. FIJI analysis: partial images of the red and green channels are shown. Yellow markings represent regions of interest (ROIs). (A) Lysotracker Red with markings for 6 selected cells for analysis; (B) pHRodo green with 6 selected cells; (C) pHRodo Green with 6 selected cells, containing markings for lysosomes; (D) pHRodo Green with 6 selected cells with deleted intensities for lysosomes; (E) pHRodo Green with 6 selected cells representing only the lysosomes.
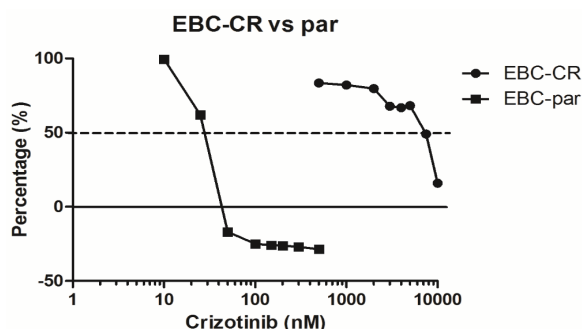

Fig. 2. Growth inhibition by crizotinib: cells were treated with a crizotinib concentration range of 0-10 μM for 72 h. Values represent mean $\pm$ SEM of triplicates of 3 separate experiments. Horizontal dashed line represents a growth inhibition of 50%. EBC-CR: crizotinib resistant line; par: parental EBC-1 cell line.

indicator. In the first step, sunitinib (5 μM, LC laboratories, Woburn, MA) and Lysotracker red (0.5 μM, Thermo Scientific) were added to the wells. The cells were incubated in the dark for 30 min at 37°C. In the second step, pHRodo green was added according to manufacturer's instructions, final concentration 1× (Life Technologies) and cells were further incubated in the dark at 37°C for 30 min. A single drug stock solution was made for treatment of all wells. Cells were then washed 3 times with PBS and imaged using a Leica TCS SP8 STED 3× microscope. A 3D representation of the cells was obtained by imaging the cells on several planes, leading to a z-stack. Z-stacks were imaged at bright field, 445 nm (laser power 2) for sunitinib, 488 nm (laser power 0.7) for pHRodo green and 561 nm (laser power 1.5) for Lysotracker Red.

Images were analyzed with FIJI-software [19–21]. Z-stacks per sample were imported with Bio-Formats. For each z-plane the following analysis was performed on 10 representative cells per sample. In the first step, lysosomes were identified using the Lysotracker Red

channel (Fig. 1A). The image of the red channel was copied and made binary. With the 'analyze particle' tool of FIJI, the lysosomes were selected using the automatic threshold 'triangle'. The regions of the lysosomes were saved. Next, the image of the pHRodo green channel was copied and the regions of the 10 cells were selected (Fig. 1B). Firstly, the regions of the lysosomes were overlaid (Fig. 1C) with this image and the intensity of these regions was erased (Fig. 1D). Then, the total intensity of the remaining regions of the cells was analyzed and saved as "intensity of cytoplasm". Secondly, the regions of the lysosomes were selected and the intensity of the outside region was erased (Fig. 1E). The intensity of the lysosomes was saved as "intensity of lysosomes". This analysis was performed for all planes of the z-stack. We summed up these intensities and corrected for the area of the cells or lysosomes respectively, and the amount of the z-planes.

3. Results

3.1. Crizotinib resistance in stepwise selected tumor subline

Selection of EBC-1 NSCLC cells in gradually increasing concentrations of crizotinib led to the establishment of the EBC-CR daughter cell line (Fig. 2). This drug resistant subline was cultured for at least 4 weeks without drugs prior to drug sensitivity assessment. The sensitivity of both the parental and drug-resistant tumor cell lines to crizotinib was determined using the SRB-assay (Fig. 2). The crizotinib IC_{50} of the parental cell line was 28.5 $\pm$ 1.1 nM, whereas the IC_{50} value of the EBC-CR subline markedly increased to 7.4 $\pm$ 0.3 μM, thus representing a 260-fold crizotinib resistance.

3.2. Tyrosine kinase activity

To determine the effect of crizotinib on downstream signaling, the kinase activity was determined in both cell lines after exposure of intact cells to crizotinib (Fig. 3) using an equally cytotoxic concentration of crizotinib. Basal tyrosine kinase activity of the EBC-CR
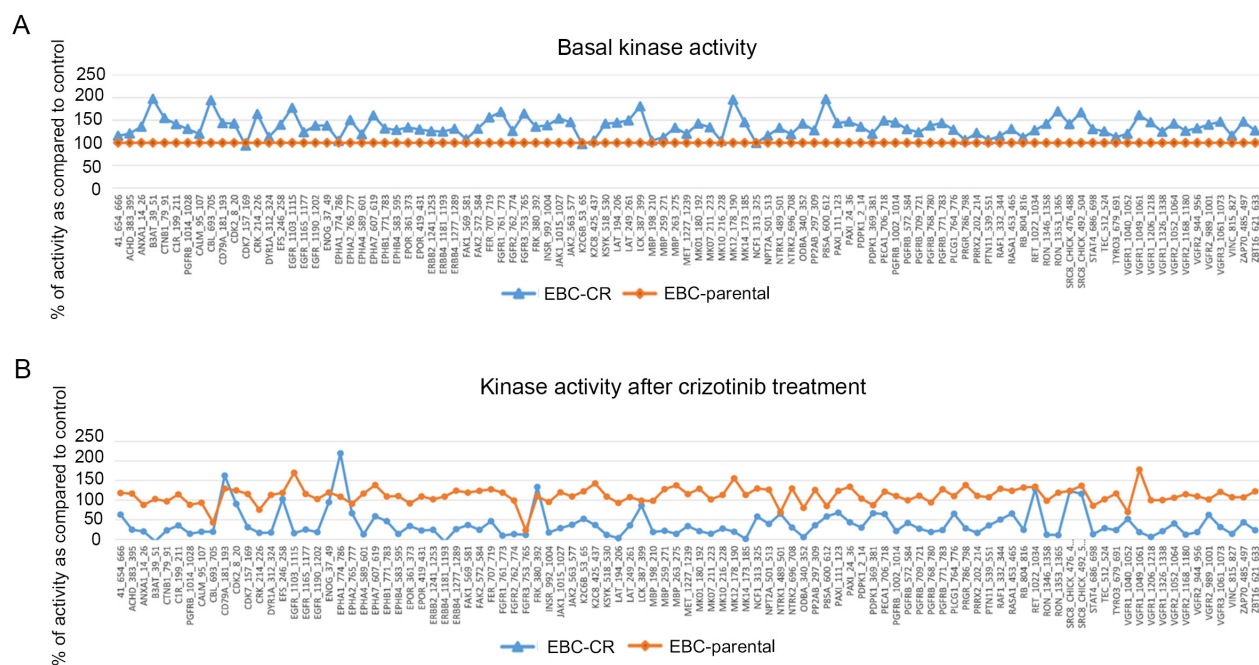
Fig. 3. Tyrosine kinase activity. Cells were treated for 24 h with their respective IC$_{50}$ values of crizotinib (25 nM for EBC-parental (orange) and 7 µM for the EBC-CR (blue)) or 0.1% DMSO as control. Cells were lysed and tyrosine kinase activity was determined with the pamgene kinase array. (A) Kinase activity of EBC-CR vs parental is represented in this graph. (B) Inhibition of kinase activity after crizotinib treatment compared to the respective basal activity of both cell lines.
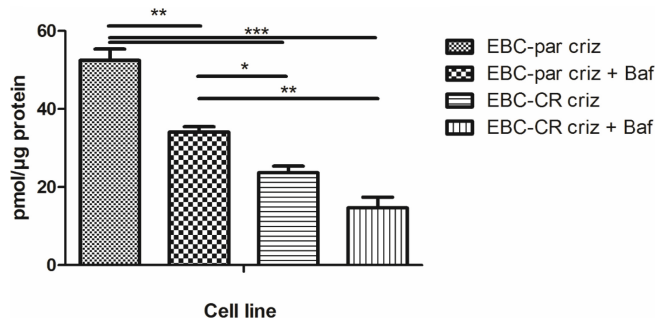

Fig. 4. Intracellular crizotinib concentrations: cells were treated for 24 h with 5 µM crizotinib. Pellets were snap-frozen and analysis was performed by liquid chromatography coupled to a tandem mass-spectrometer. EBC-par: parental EBC-1 cell line; EBC-CR: crizotinib resistant EBC-1 daughter cell line. Baf: 50 nM Bafilomycin, added 30 min before crizotinib treatment. *: $p < 0.05$; **: $p < 0.01$; ***: $p < 0.001$.

versus parental EBC-1 cells showed an overall higher kinase activity as compared to the basal activity (black) in the parental cell line, which was set at 100% for each kinase. This increased activity was approximately 2-fold higher for the following kinases: B3AT (Band-3 cotransporter, an anion transporter), c-Cbl (Casitas B-lineage lymphoma), CRK, DYR1A (Dual specific tyrosine phosphorylation-regulation kinase), Fes, LCK and p85A. In the parental cell line its kinase activity was not inhibited in response to crizotinib treatment, whereas in the EBC-CR resistant cell line, this kinase activity dropped below the background level [22]. C-Cbl is the E3-ligase that is responsible for marking several tyrosine kinase receptors, including cMET and EGFR, for breakdown [23]. This kinase was

inhibited after crizotinib treatment in both the parental and resistant cell lines. CRK [24], Fes [25] and LCK [26] are downstream signaling proteins that were all inhibited after crizotinib treatment in both cell lines. The PI3K subunit p85A was also inhibited by crizotinib treatment. After crizotinib treatment, a 2-fold increase in EphA1 (Ephrin receptor type A) activity was observed in EBC-CR cells. Activation of this receptor leads to increased adhesion to the extracellular matrix [27]. cMET activity was inhibited in both cell lines after crizotinib treatment. This inhibition was stronger in the EBC-CR as compared to the parental cell line.

3.3. Intracellular concentration of crizotinib

In the parental cell line, 24 h treatment with 5 µM crizotinib resulted in a mean intracellular crizotinib concentration of 52.5 pmol/µg protein (Fig. 4). Whereas, in the resistant cells, this intracellular concentration dropped by 55% with an intracellular level of 23.5 pmol/µg protein ($p < 0.001$). The addition of the V-ATPase inhibitor bafilomycin A1 (which alkalinizes the native acidic pH of lysosomes) prior to crizotinib treatment led to a ∼40% decrease in the intracellular concentrations of crizotinib in both the parental cells and their drug resistant subline with values of 34.1 and 14.7 pmol/µg protein, respectively.

3.4. Intracellular effect of crizotinib

The pH sensitive pHRodo Green probe was used to assess the intracellular pH in the different cellular compartments. Bright staining correlates with acidic pH whereas alkalinization results in markedly decreased fluorescence. Lysotracker Red specifically stains the lysosomes and sunitinib was used to visualize lysosomal sequestration of weak-base small molecule protein tyrosine kinase inhibitors. The

Panel 1: EBC-parental; 0.1% DMSO
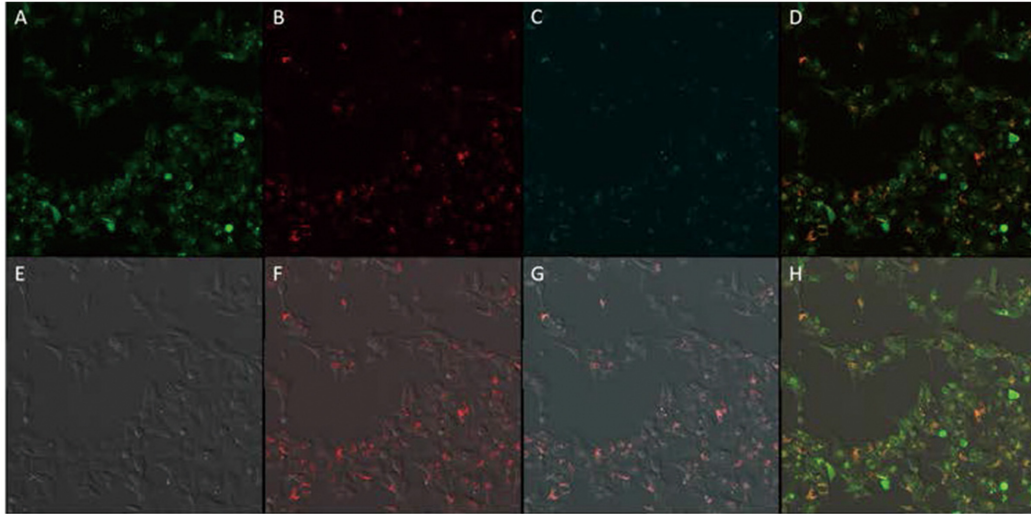
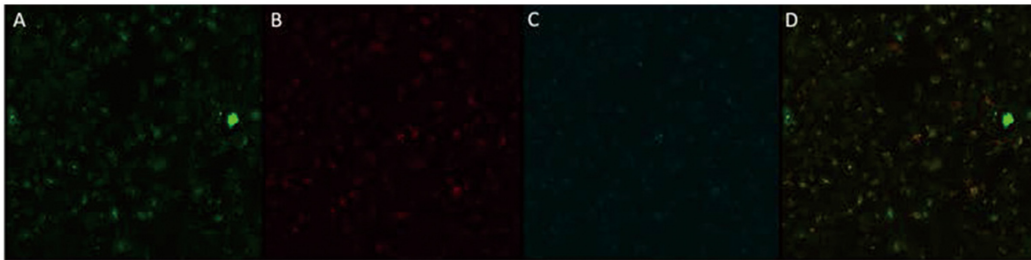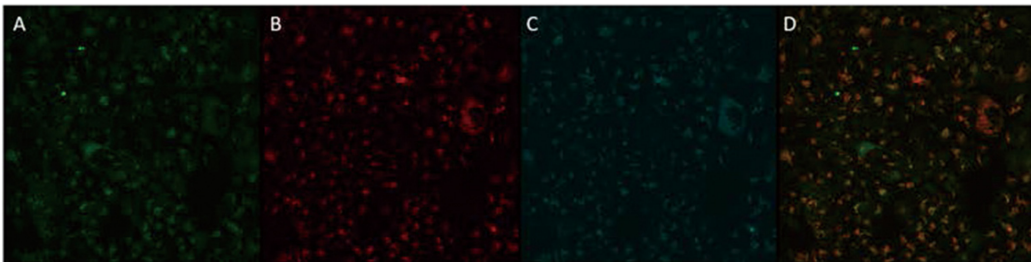Panel 2: EBC-parental; 5 µM crizotinib
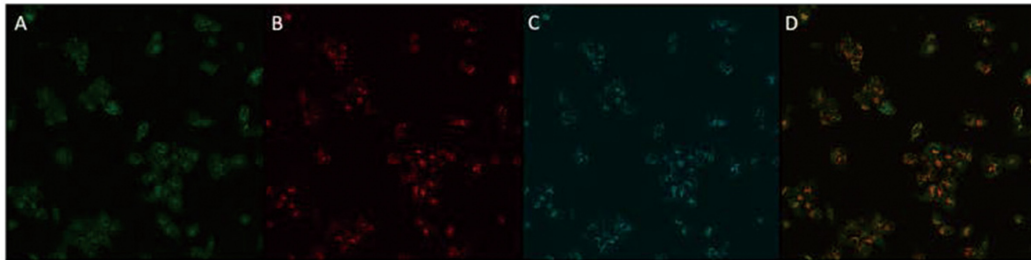
Panel 3: EBC-CR; 0.1% DMSO

Panel 4: EBC-CR; 5 µM crizotinib

Fig. 5. Intracellular effect of crizotinib: cells were seeded in a chambered cover glass and treated with drugs for 24 h. Cells were stained with sunitinib and Lysotracker red for 1h and with pHRodo Green for 30 min. Cells were imaged in depth by dividing them in different layers (z-stack). Z-stacks were imaged using a Leica TCS SP8 STED 3× microscope. (A) pHRodo Green; (B) Lysotracker red; (C) Sunitinib; (D) pHRodo Green + lysotracker red overlay; (E) Bright field; (F) Bright field + lysotracker red overlay; (G) Bright field, lysotracker red and sunitinib overlay; (H) Bright field, lysotracker red and pHRodo Green overlay. Representative images of one z-plane.

first panel of Fig. 5 shows representative images from the different channels and overlays of the parental EBC-1 cell line treated with DMSO. The images of Lysotracker red (Fig. 5B) and sunitinib (Fig. 5C) are shown to overlap in the first panel of Fig. 5G. The

bright field image also shows that these lysosomes are located in the peri-nuclear zone (Fig. 5G). An overlay of Lysotracker red and pHRodo Green co-localizes at the lysosomes in the brightest spots of pHRodo Green (Fig. 5D, 5H). The second panel shows the parental

EBC-1 cell line after treatment with 5 μM crizotinib. The number of fluorescent events in the lysotracker red and sunitinib channel were increased in comparison with the control. The EBC-CR crizotinib resistant cell line (third and fourth panels) showed the same effect after crizotinib addition. Quantification of the average fluorescence intensity of 10 cells throughout the stacks is shown in Fig. 6. The intensity of pHRodo Green was quantified in the cytoplasm and in the lysosomes in both cell lines. The parental EBC-1 cell line showed a basal intensity of 1637 RFU (relative fluorescence units) in the cytoplasm and 3862 RFU in the lysosomes. After treatment with crizotinib, the intensity of pHRodo Green doubled in the cytoplasm and in the lysosomes. pHRodo Green fluorescence intensity in the cytoplasm and in the lysosomes is similar to the values in the parental cell line after crizotinib treatment. Treatment with crizotinib did not increase the fluorescence intensity in the cytoplasm but did significantly decrease the fluorescence intensity of the lysosomes. In summary, crizotinib increased the fluorescence intensity in both the cytoplasm and lysosomes in parental cells, whereas in the resistant cell subline the fluorescence intensity of the lysosomes was significantly decreased. This points towards a general acidification in the parental cell line, whereas in the resistant subline the lysosomes became more alkaline when pulse treated with crizotinib.

4. Discussion

In this study we established a cMET gene amplified cell line that is highly resistant to the cMET-TKI crizotinib. Growth inhibition assays after 4 weeks of drug-free culturing, showed a 260-fold resistance of the EBC-CR daughter cell line as compared to its parental EBC-1 cell line.

The impact of crizotinib on the tyrosine kinase activity was determined using a tyrosine kinase activity array. Remarkably, overall inhibition of tyrosine kinase activity by crizotinib was the strongest in the EBC-CR cell line, which can be explained by the much higher, although isocytotoxic concentration of 7 μM crizotinib, as compared to the 25 nM used for the parental cell line. Addition of crizotinib to the parental cell line led to a slight increase of ∼20% in most tyrosine kinases. Only a few exceptions were observed: c-CBL, FGFR3 and NTRK. Since c-CBL is the E3-ubiquitin ligase responsible for cMET degradation [23], a decrease in cMET activity can explain a decrease in c-CBL activity. The other receptors FGFR3 and NTRK are not described to be inhibited by crizotinib. Although, even with the low concentration of 25 nM, the inhibition is as strong as compared to the effect of the high 7 μM concentration. The B3AT anion transporter showed complete inhibition in the resistant cell line after crizotinib treatment, whereas in the parental cell line its activity remained unchanged. This transporter is known to be active in lung tissue, where it pumps HCO_3^- into the cell in exchange for Cl^-. In the cells, H^+ binds to $HCO3^-$ resulting in the generation of CO_2 and H_2O [22].

Other possible mechanisms of crizotinib resistance are mutations in cMET. Two resistance mutations have been described in the case of cMET exon 14 skipping. The D1228N mutation confers acquired resistance towards crizotinib [6], whereas the Y1230C mutation confers intrinsic resistance to crizotinib [28]. However, in the case of cMET gene amplification, no resistance mutations in cMET have been described thus far. If a resistance mutation was present in cMET, a rise in kinase activity or continuous cMET signaling would be expected, whereas the kinase activity of cMET is inhibited more
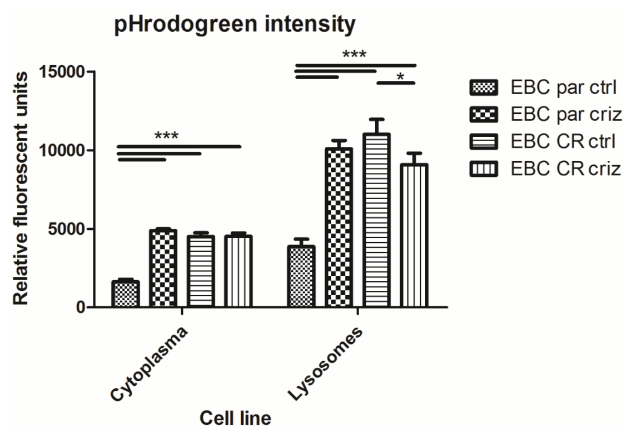

Fig. 6. Subcellular pHRodo Green fluorescence intensity: cells were treated with crizotinib for 24 h and stained with pHRodo Green, lysotracker red and sunitinib as described in Fig. 5. Analysis with FIJI was performed, selecting the lysosomes based on lysotracker red staining and determining the intensity of pHRodo Green in the cytoplasm and the lysosomes respectively for all z-planes of the stack, while taking into account the cell area and number of stacks for each sample. EBC par: parental cell line; EBC CR: crizotinib resistant daughter cell line; ctrl: DMSO treated cells; criz: treated with 5 μM crizotinib. *: $p < 0.05$; **: $p < 0.01$; ***: $p < 0.001$.

significantly in the resistant cell line as compared to the parental cell line.

Given that crizotinib is a hydrophobic weak base drug, lysosomal sequestration emerges as a viable possibility as an underlying mechanism of drug resistance [11]. A previous study from our lab showed that crizotinib is indeed sequestered in lysosomes [29]. In the current study, we found that the intracellular concentration of crizotinib was significantly lower in the resistant cell line as compared to the parental cell line. Lysosomal sequestration has been described for sunitinib [30], whereby it enables cells to transiently tolerate sunitinib, raising the IC_{50} value 2-fold. In this study of Gotink et al., the cells were transiently resistant to sunitinib, but regained sensitivity after 12 weeks of culturing in drug-free medium [13]. However, our data showed a decrease in crizotinib concentration in the resistant cell line. Therefore, we aimed to visualize the lysosomes and drug sequestration, using the autofluorescent drug sunitinib. These results showed that crizotinib increased the amount of lysosomes in both sensitive and resistant EBC-1 cells. The key element for lysosomal drug sequestration is the pH gradient between the cytoplasm and the lysosomes. Under normal physiological conditions, the pH of the cytoplasm is expected to range between pH 7.2-7.4, whereas the lysosomes are much more acidic with a pH around 5. When this gradient becomes smaller, lysosomal drug sequestration is deregulated, leading to a decrease or increase of intracellular drug concentration. Several cell lines have been described with a distorted pH-gradient, leading to a narrower gradient in case of MCF-7 and HL-60 cells [31]. Therefore, we used the pH sensitive pHRodo Green probe during our live cell imaging studies in order to monitor the subcellular pH in the EBC-CR and EBC-parental cell lines. Quantification of the fluorescence intensity of this probe showed that after treatment with crizotinib, a decrease in the pH of both the cytoplasm and the lysosomes was detectable in parental cells. In contrast, the pH of the cytoplasm in the EBC-CR remained stable, but the lysosomes became significantly less acidic. It should be noted that in the untreated EBC-CR

cells the pH was already as low as in the treated EBC-parental cells, pointing towards a permanent change in pH in the EBC-CR cells. This permanent acidification of the lysosomes might offer immediate protection against crizotinib for these cells, and thus contribute to crizotinib resistance. This permanent change might be caused by an increased expression of the V-ATPase, although this theory needs to be confirmed *in vitro*.

Focusing on the intracellular crizotinib concentration, a lower concentration of crizotinib was observed in EBC-CR cells as compared to parental EBC-1 cells. This concentration of crizotinib decreased after addition of bafilomycin A1 in both cell lines, showing that acidification of the lysosomes did play a role in crizotinib sequestration in both cell lines. The decreased crizotinib concentration in the EBC-CR cell line might be explained by an upregulation of its efflux pump: P-glycoprotein [32, 33]. Another possibility is that the increased lysosomal acidification leads to faster and increased crizotinib sequestration. This might in turn lead to upregulation of lysosomal exocytosis in the EBC-CR as compared to the EBC-parental cell line; anticancer drug-induced lysosomal biogenesis and exocytosis was recently shown [14, 15]. More research is needed to elucidate the exact mechanism of the decreased crizotinib concentration in the EBC-CR cells.

In conclusion, the impaired sequestration of crizotinib in EBC-CR cells, together with the increased acidification of the lysosomes, appear to contribute to crizotinib resistance in a cMET-amplified NSCLC cell line.

Acknowledgments

Conflict of Interest

The authors declare no conflict of interest.

References

[1] Van Der Steen N. *et al*. cMET in NSCLC: Can we cut off the head of the Hydra? From the pathway to the resistance. *Cancers*, 2015; 7: 556-573.

[2] Van Der Steen N, *et al*. cMET exon 14 skipping: from the structure to the clinic. *J Thorac Oncol*, 2016; 11: 1423-1432.

[3] Jenkins RW, *et al*. Response to Crizotinib in a Patient With Lung Adenocarcinoma Harboring a MET Splice Site Mutation. *Clin Lung Cancer*, 2015; 16: e101-e104.

[4] Awad MM, *et al*. MET Exon 14 Mutations in Non-Small-Cell Lung Cancer Are Associated With Advanced Age and Stage-Dependent MET Genomic Amplification and c-Met Overexpression. *J Clin Oncol*, 2016; 34: 721-30.

[5] Engelman JA, *et al*. MET amplification leads to gefitinib resistance in lung cancer by activating ERBB3 signaling. *Science*, 2007; 316: 1039-1043.

[6] Heist RS, *et al*. Acquired Resistance to Crizotinib in Non-small Cell Lung Cancer with MET exon 14 skipping. *J Thorac Oncol*, 2016; 11: 1242-1245.

[7] Pao W, *et al*. Acquired resistance of lung adenocarcinomas to gefitinib or erlotinib is associated with a second mutation in the EGFR kinase domain. *PLoS Med*, 2005; 2: 0225-0235.

[8] Wang S, Tsui ST, Liu C, Song Y & Liu D. EGFR C797S mutation mediates resistance to third-generation inhibitors in T790M-positive non-small cell lung cancer. *J Hematol Oncol*, 2016; 9: 59.

[9] Linardou H, *et al*. Assessment of somatic KRAS mutations as a mechanism associated with resistance to EGFR-targeted agents: a systematic review and meta-analysis of studies in advanced non-small-cell lung cancer and metastatic colorectal cancer. *Lancet Oncol*, 2008; 9: 962-972.

[10] Sequist LV, *et al*. Genotypic and histological evolution of lung cancers acquiring resistance to EGFR inhibitors. *Sci Transl Med*, 2011; 3: 75ra26.

[11] Zhitomirsky B & Assaraf YG. Lysosomes as mediators of drug resistance in cancer. *Drug Resist Updat*, 2016; 24: 23-33.

[12] Zhitomirsky B & Assaraf YG. The role of cytoplasmic-to-lysosomal pH gradient in hydrophobic weak base drug sequestration in lysosomes. *Cancer Cell Microenviron*, 2015; 2: 3-9.

[13] Gotink KJ, *et al*. Lysosomal sequestration of sunitinib: A novel mechanism of drug resistance. *Clin Cancer Res*, 2011; 17: 7337-7346.

[14] Zhitomirsky B & Assaraf YG. Lysosomal sequestration of hydrophobic weak base chemotherapeutics triggers lysosomal biogenesis and lysosome-dependent cancer multidrug resistance. *Oncotarget*, 2015; 6: 1143-56.

[15] Zhitomirsky B & Assaraf YG. Lysosomal accumulation of anticancer drugs triggers lysosomal exocytosis. *Oncotarget*, 2017; 8: 45117-32.

[16] Keepers YP, *et al*. Comparison of the Sulforhodamine B Protein and Tetrazolium (MTT) assays for *in vitro* chemosensitivity testing. *Eur J Cancer*, 1991; 27: 897-900.

[17] Galvani E, *et al*. Molecular mechanisms underlying the antitumor activity of 3-aminopropanamide irreversible inhibitors of the epidermal growth factor receptor in non-small cell lung cancer. *Neoplasia*, 2013; 15: 61-72.

[18] Honeywell R, *et al*. Simple and selective method for the determination of various tyrosine kinase inhibitors used in the clinical setting by liquid chromatography tandem mass spectrometry. *J Chromatogr B Anal Technol Biomed Life Sci*, 2010; 878: 1059-1068.

[19] Schindelin J, *et al*. Fiji: an open-source platform for biological-image analysis. *Nat Methods*, 2012; 9: 676-682.

[20] Schindelin J, Rueden CT, Hiner MC & Eliceiri KW. The ImageJ ecosystem: An open platform for biomedical image analysis. *Mol Reprod Dev*, 2015; 82: 518-529.

[21] Schneider CA, Rasband WS & Eliceiri KW. NIH Image to ImageJ: 25 years of image analysis. *Nat Methods*, 2012; 9: 671-675.

[22] Reithmeier RAF, *et al*. Band 3, the human red cell chloride/bicarbonate anion exchanger (AE1, SLC4A1), in a structural context. *Biochim Biophys Acta – Biomembr*, 2016; 1858: 1507-1532.

[23] Petrelli A, *et al*. The endophilin-CIN85-Cbl complex mediates ligand-dependent downregulation of c-Met. *Nature*, 2002; 416: 187-190.

[24]   Feller SM. Crk family adaptors-signalling complex formation and bio-
       logical roles. *Oncogene*, 2001; 20: 6348-71.

[25]   Li J, Smithgall TE, Li J & Smithgall TE. Fibroblast Transformation
       by Fps / Fes Tyrosine Kinases Requires Ras , Rac , and Fibroblast
       Transformation by Fps / Fes Tyrosine Kinases Requires Ras , Rac , and
       Cdc42 and Induces Extracellular Signal-regulated and c-Jun N-terminal
       kinase activation. *J Biol Chem*, 1998; 273: 13828-13834.

[26]   Cuevas B, *et al*. SHP-1 regulates Lck-induced phosphatidylinositol 3-
       kinase phosphorylation and activity. *J Biol Chem*, 1999; 274: 27583-
       27589.

[27]   Pasquale EB. Eph receptors and ephrins in cancer: bidirectional sig-
       nalling and beyond. *Nat Rev Cancer*, 2010; 10: 165-180.

[28]   Ignatius Ou S-H, *et al*. Emergence of pre-existing MET Y1230C muta-
       tion as a resistance mechanism to crizotinib in NSCLC with MET exon
       14 skipping. *J Thorac Oncol*, 2016; 12: 137-140.

[29]   Da Silva CG, Honeywell RJ, Dekker H & Peters GJ. Physicochemical
       properties of novel protein kinase inhibitors in relation to their substrate
       specificity for drug transporters. *Expert Opin Drug Metab Toxicol* 2015;
       11: 703-717.

[30]   Gotink KJ, *et al*. Cross-resistance to clinically used tyrosine kinase
       inhibitors sunitinib, sorafenib and pazopanib. *Cell Oncol* 2015; 119-129.

[31]   Larsen AK, Escargueil AE & Skladanowski A. Resistance mechanisms
       associated with altered intracellular distribution of anticancer agents.
       Pharmacol Ther, 2000; 85: 217-229.

[32]   Chuan Tang S, *et al*. Increased oral availability and brain accumu-
       lation of the ALK inhibitor crizotinib by coadministration of the P-
       glycoprotein (ABCB1) and breast cancer resistance protein (ABCG2)
       inhibitor elacridar. *Int J Cancer*, 2014; 134: 1484-1494.

[33]   Katayama R, *et al*. P-glycoprotein Mediates Ceritinib Resistance in
       Anaplastic Lymphoma Kinase-rearranged Non-small Cell Lung Cancer.
       EBioMedicine 2016; 3: 54-66.